Metal-in-metal localised surface plasmon resonance

G B Smith and A E Earp
Department of Physics and Advanced Materials and Institute of Nanoscale Technology, University of Technology, Sydney
PO Box 123, Broadway NSW 2007 Australia
email: g.smith@uts.edu.au

Abstract. Anomalous strong resonances in silver and gold nano-porous thin films which conduct are found to arise from isolated metal nano-islands separated from the surrounding percolating metal network by a thin loop of insulator. This observed resonant optical response is modelled. The observed peak position is in agreement with the observed average dimensions of the silver core and insulator shell. As the insulating ring thickness shrinks the resonance moves to longer wavelengths and strengthens. This structure is the Babinet's principle counterpart of dielectric core-metal shell nanoparticles embedded in dielectric. Like the latter tuning of resonant absorption is possible, but here the matrix reflects rather than transmits and tuning to longer wavelengths is more practical. A new class of metal mirror for a single thin layer is identified using the same resonances in dense metal mirrors. Narrow band deep localised dips in reflectance result.

1. Introduction

Surface plasmon resonance (SPR) in conducting nanoparticles has enabled many recent advances in optical nanoscience and related nanotechnology. The metal or transparent conductor nanoparticles are usually dispersed in an insulating medium to achieve their special optical response, which depends on the particle's plasma frequency ω_p and its shape. These systems are thus mostly transmitting at visible and NIR wavelengths, apart from this narrow SPR absorption band. Their SPR moves from visible wavelengths into the NIR as ω_p decreases. We show here that a sharp local SPR at NIR wavelengths within an electrically conducting, thin reflective layer is also possible. Prior analyses of experimental data in terms of such resonances does not appear to have been previously reported. Their signature however exists in select historical thin film optical data, for example in the paper on very thin nanoporous gold by Smith et al [1]. We also present new evidence using films made especially for this study. Old and new experimental evidence in select random nanoporous-systems and supporting models are thus one main aspect of this report. However the main outcome and future interest may be in what these new models predict when the matrix is a thin dense metal layer. The resulting prospects for a new class of optical response and thin film technology will be outlined. Such structures are feasible using a variety of production techniques. The central entity of interest embedded within a thin film is illustrated in figure 1. The matrix can be a dense or porous conducting network. As illustrated in figure 1 the inclusion has 2-dimensional symmetry which seems most suited to the observed

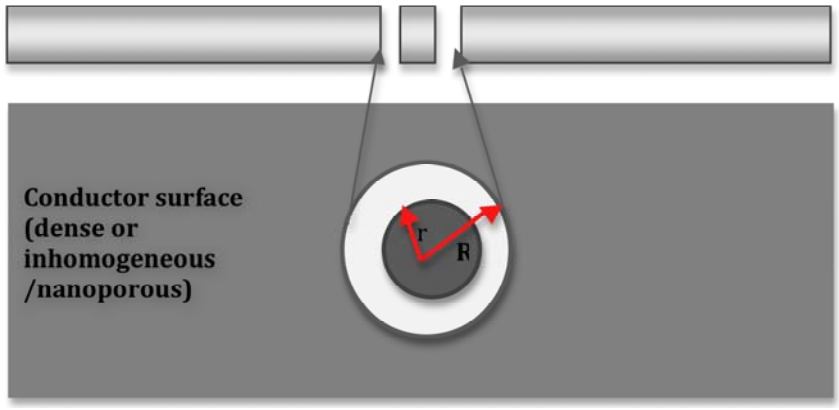

Figure 1. Section view (top) and an expanded plan view (bottom) for an average SPR resonant entity in a thin conducting layer. A nano- annulus of insulator is wrapped around an isolated circular cylinder metal island embedded in either a metal thin film, or a porous conductor which is optically homogeneous.

structures whose optical response is analysed in this paper. The models following apply equally well to 3-dimensional core-shell inclusions, for example an insulator coated metal nanoparticle completely buried under metal. The ability to simply add sharp resonant absorption to a reflector's optical response opens up exciting new opportunities in thin film and metal optics, and in plasmonics.

We will introduce here experimental evidence for this class of SPR's in gold and silver random nanoporous metal layers, as that was the context in which we first discovered them. The examples used in this paper arose naturally during film growth. That finding prompted us to subsequently deliberately synthesise layers of oxide coated metal nanoparticles with a range of oxide thicknesses, then completely bury them under dense metal to check features of these metal-in-conductor resonances in a different and more controlled 3-dimensional context. That is a major study in its own right so it will follow separately. However it is worth noting that the distinct resonant features in that class of films are also as predicted by the basic models we will now introduce when adjusted for the different nanostructure and the matrix of dense rather than porous metal.

Nanoporous conducting layers have been produced by two quite distinct methods; one by direct deposition of very thin layers, and one made via a chemical etching route. Different nanostructures arise and in both cases the conducting network is disordered with isolated pores. The resonant entities of interest here lie within this network. It is well known that growing noble metal films evolve from isolated nano-islands, to percolating nanoporous networks which conduct, and finally to fully dense thin films [1-3]. In the transition zone from islands to locally conducting network, nano-islands and linked material will co-exist, and it is thus quite likely that some islands can stand alone within the more extended network. These are the entities which

generate anomalous NIR absorption. Without them the nanoporous or granular conductors behave optically like a standard metal but with a lower plasma frequency and higher loss than their dense parent [4]. Reflectance in the absence of these additional core-ring structures is thus that of a classical Drude conductor and rises smoothly to a high level as wavelength increases from a floor within the visible or the NIR. The anomalous absorption introduces distinct structure into such spectra. An additional consideration with smooth metal is that SPR resonant void structures in smooth, dense metal films may generate extended surface charge waves or polaritons before the local SPR fields are dissipated as heat. This issue may be of interest in its own right for some metal-in-dense metal structures, but not all. However extended surface polaritons are not an issue in the nanoporous disordered conductors used in this study, due to surface disorder and scattering. Evidence has previously been reported that polaritons are not present or weak [5] on the outer surfaces of disordered nanoporous gold conductors. This assumption is supported by the combination of observations and models that follow.

The metal core-insulator ring resonant position is widely tuneable in silver and gold, mainly across the NIR but also in the visible, by simple modifications of the entity's structure without altering its shape. It appears that the resonant quality or Q-factor can in practice be much higher than that obtainable in known insulator core/metal shell (Babinet's principle) counterparts, which are also tuneable. Most reports on these have been on 3-dimensional structures [6,7]. [Babinet's principle in 2d involves swapping metal for insulator and vice versa in the structure]. The insulator-core in metal-shell, all embedded in an insulator, have been of interest for tunability and the strong local fields they generate [5-8]. Due to limits on how thin metal shells with good electrical quality can be made the tuning range of that system is unfortunately quite limited in practice [7]. The resonator in this study may be tuneable in practice over a much wider range than the metal shell case since thinner dielectric shells on metals seem to be more easily fabricated. In our growing thin films examples of very thin dimensions of the voids around the metal seem to arise (examples below).

2. Local surface plasmon resonance in metal thin films : theory

The structure illustrated in figure 1 provides the basis for the optical models that explain observed esonant data on select nanoporous metal layers. The following analysis is done in the quasi-static limit since wavelength is very much larger than the resonant entity scale, which is typically 14 to 16 nm in radius. The polarisability α of the entity in figure1 generalised for arbitrary shape, and for electric fields in the film plane can be written down compactly in terms of an effective combined dielectric constant ε_{MG} for the silver core/insulating shell combination as seen externally which is given in equation (1). This nomenclature is deliberate as ε_{MG} is exactly what would be obtained for the effective dielectric constant in the Maxell Garnett effective medium model of a random array of metal embedded in the insulator. For the 2-d case area and volume fill factor f are given by $f \quad \frac{r^2}{R^2}$, while in 3-d $f \quad \frac{r^3}{R^3}$.

$$MG \quad h \quad \frac{Ag \quad h(\frac{1}{L} \quad 1) \quad f(\frac{1}{L} \quad 1)(Ag \quad h)}{Ag(1 \quad f) \quad h\frac{1}{L} \quad 1 \quad f} \qquad (1)$$

The dielectric constants are ε_{Ag} for silver and ε_h for the insulating ring. L is a general depolarisation factor which we confine for the 2-d analysis to L = 0.5. For spheres in 3-d, L =1/3. The polarizability of the core-shell entity embedded in dense silver becomes in general

$$A\frac{1}{L}_{Ag}\frac{MG \quad Ag}{MG \quad (\frac{1}{L} \quad 1)_{Ag}} \tag{2}$$

with A the core-shell inclusion area if 2-dimensional or volume if 3-d. If embedded in nanoporous silver ε_{Ag} is replaced by the effective ε_m* for the nanoporous metal, which for this study mainly involves the effective Drude response [4] .

The extra absorption arises because reflectance drops in the resonant zone when these structures are present. That is more light enters the structure. As this is a plasmonic material at these wavelengths another way of analysing the extra absorption is in terms of an homogenised effective medium for the whole system, with complex effective indices (n*, k*) satisfying $(n^* \quad ik^*) \quad \sqrt{\quad^*}$. The homogenised complex dielectric constant $\varepsilon^* = \varepsilon_1^* + i\varepsilon_2^*$ is given by equation (3), assuming low volume fraction q of defects as observed. This limit enables us to focus in this introduction on isolated entity resonances, though interactions between entities at larger q can be included by using classical effective medium forms.

$$^* \quad _{Ag} \quad 1 \quad 2q\frac{_{MG}(f) \quad _{Ag}}{_{MG}(f) \quad _{Ag}} \tag{3}$$

In figures 2(a) and 2(b) with q = 0.05 and L = 0.5 this model predicts classical narrow SPR absorption bands at each f value with $\varepsilon_2^*(\lambda)$ having sharp peaks sitting on top of the smooth curve for the enclosing metal, for example on top of either $\varepsilon_{2,Ag}(\lambda)$ or $\varepsilon_{2,m}^*(\lambda)$. Known bulk values for gold and silver [10] were used in these models. Corrections to the Drude term for increased relaxation rates in the core metal-islands and in the surrounding film are added when appropriate, that is to the particle in these plots but not the dense matrix. When we consider porous matrices an enhanced relaxation rate is used in $\varepsilon_{2,m}^*(\lambda)$ as well as in the particle. It can be found experimentally [4].

There is clearly a very strong modulation of the metallic dielectric response. Likewise the classical double peak structure at resonance in $\varepsilon_1^*(\lambda)$ now sits astride, for a dense silver matrix $\varepsilon_{1,Ag}(\lambda)$ as in figure 2(b), or for a porous matrix $\varepsilon_{1,m}^*(\lambda)$. This spectrally dependent base-line for resonant peaks is a distinguishing feature of metal-in-metal resonance when compared with metal-in-dielectric SPR absorption peaks. The latter sit on a base-line which is relatively constant with wavelength. Figures 3(a), and3(b) compare the same set of results for gold which has a similar plasma frequency to silver but higher relaxation rate and lower energy inter-band terms. These both impact as seen on the final resonant structure. Gold-in-gold thus has broader and red shifted resonant peaks compared to silver-in-silver. Both show local regions of very large increases in the extent to which $\varepsilon_1^*(\lambda)$ goes negative, though in silver this dip is much more pronounced. Such a large negative dip might for example be of use in constructing negative index materials, or for enhanced shielding though enhanced loss is an issue.

The homogenized complex indices n*, k* can also be derived from equation (3) and have also been extracted from our spectral optical data in the NIR for layers displaying these anomalous resonances. Similar data on k*(λ) for growing silver and gold films has been reported at various times in the past [e.g. refs.1, 9] but key features produced by these resonances were not explained.

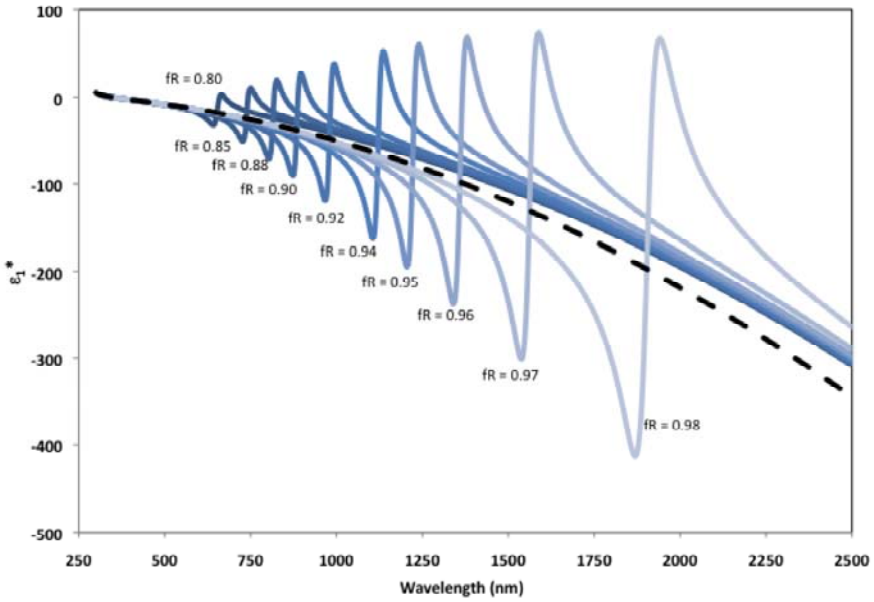

Figure 2(a) $\varepsilon_1^*(\lambda)$ for a silver core/void ring in a dense silver thin film at different $f = (r/R)^2$. The volume density of inclusions q = 0.05. The dashed line is for dense silver.

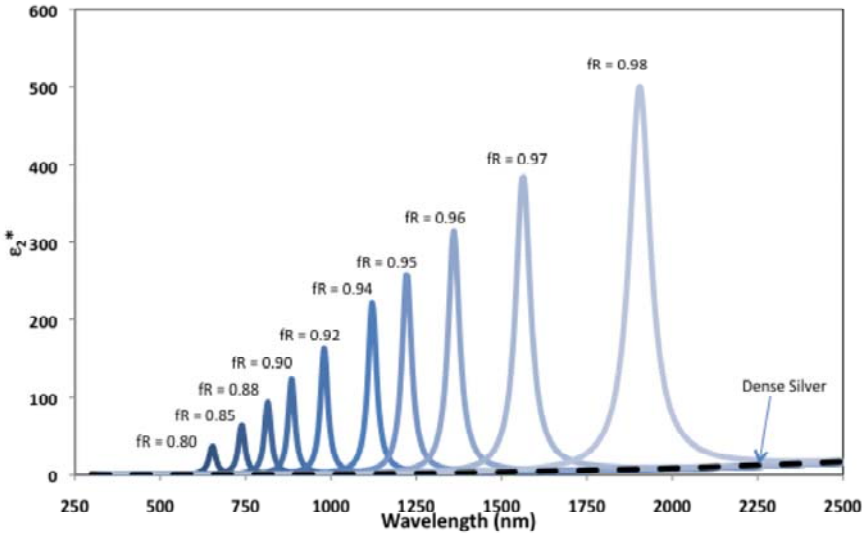

Figure 2(b) $\varepsilon_2^*(\lambda)$ for a silver core/void ring in a dense silver thin film at different $f = (r/R)^2$. The volume density of inclusions q = 0.05. The dashed line is for dense silver.

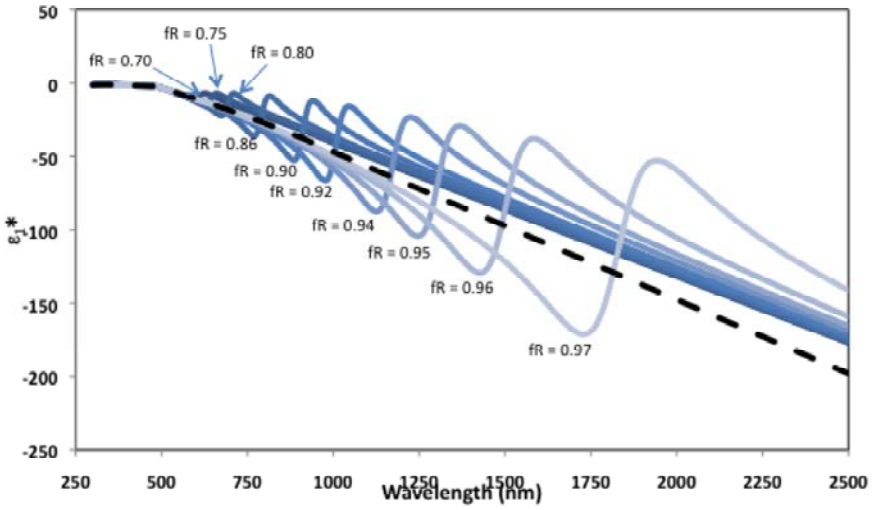

Figure 3(a) $\varepsilon_1^*(\lambda)$ for a gold core/void ring in a dense gold thin film at different $f = (r/R)^2$. Volume density of inclusions q = 0.05. The dashed line is for dense gold.

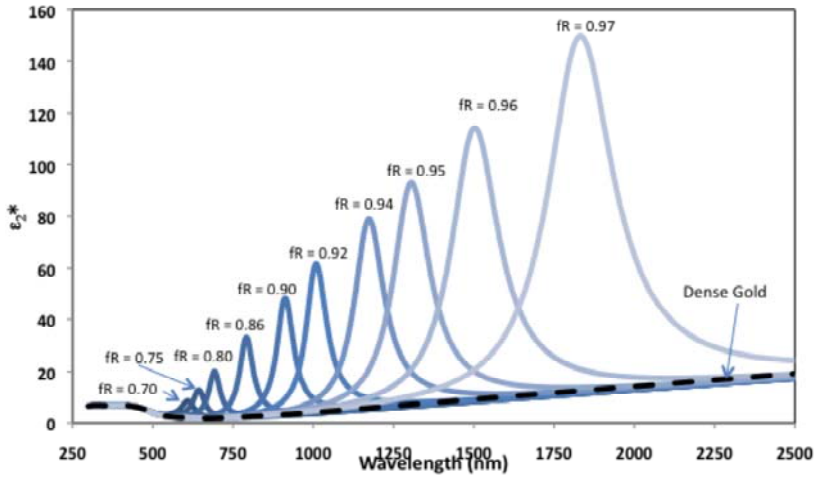

Figure 3 (b) $\varepsilon_1^*(\lambda)$ for a gold core/void ring in a dense gold thin film at different $f = (r/R)^2$. Volume density of inclusions q = 0.05. The dashed line is for dense gold.

Corrections arising from enhanced losses in the porous matrix will broaden these resonances to some extent but the main conclusions are not affected. The gold spectra are broader and less intense than silver due to its higher relaxation frequency (0.09 eV in gold films versus 0.02 to 0.03 eV in silver films). We have observed relaxation rates just above 0.02 eV in epitaxial silver layers around 12 nm thick. Practical Au or Ag shells under 6 nm thick, if achievable on an insulator nano-core will have relaxation rates much higher than these and hence much broader

and weaker resonances. The void and insulator shells we have observed in the experimental films are in contrast down to 1 nm thick and slight variations in their thickness or density are of far less concern than for metal shells.

The thick lines in the $_1$*( ) plots are from overlap of neighbouring resonances, however after summing a continuum of such resonances the result is close to this overlap line. This is qualitatively what occurs in the experimental systems we now address. The exact location of this thick curve depends on the value of q and ε_m* of the matrix. The distribution of f values will be localised around the peak wavelength and a kink in the experimental $_1$*( ), $_2$*( ) curves occurs near the peak wavelength. This is just what is observed in the disordered layers. The kink however occurs above a higher $_1$( ) plot than that for dense silver due to the surrounding conducting network being nanoporous.

The ability to tune the resonance position via control of the core-shell relative dimensions, is striking. Resonance location with void rings is very sensitive to small changes in $(r/R)^2$ once it is above 0.85 which it is for much of the experimental data in this system. For example in silver a change from f =0.92 (or r/R = 0.959) to f = 0.94 (r/R = 0.969) shifts the resonance peak by 200 nm. We shall see that once the voids are filled with an insulator this sensitivity is further enhanced, as all resonances then shift to longer wavelength. However in the data this sensitivity means that in most systems, especially random ones like those under consideration, an admix of resonances is guaranteed.

The strength of the resonance is due to the impact of the surrounding silver matrix which has a large but negative $_1$ value at these wavelengths. This makes it stronger than the insulator core-metal shell buried in insulator. The response of this Babinet's counterpart is obtained simply by swapping around $_{Ag}$ and $_h$ in equations (1-3). This swap clearly yields the same denominator apart from a change in sign and hence SPR wavelengths at each f value are identical. It is the resonant magnitudes that are different. This is because $_1$ for an insulating matrix is much smaller in magnitude than its silver counterpart. If the voids around the metal core are filled with oxide, as they are when the film is over-coated, the model resonant spectra are red shifted. Most relevant historical data on growing films has voids. Our new over-coated experimental examples in the next section are there to demonstrate the strong impact of an insulator matrix in place of voids on the metal-in-metal resonance. Doing this brought them out in the open, while in the historical void case they were less obvious The metal inclusion is now a solid insulator ring around the isolated silver island. The data for this case, and its red shift relative to having voids, adds weight to the assertion that these anomalies arise from plasmonic nanostructures.

3. Experimental Evidence

A distinct anomalous absorption band in the NIR was first observed recently in mesoporous gold [5, 11, 12]. These films were made by etching Al from thin Au-Al alloy layers. The anomalous absorption peaks in three distinct films were all centred at 1.4 eV (0.886 μm), but were of different peak strength and width. The tentative explanation at that time was either surface states or impurity states, but this option was not supported by subsequent analysis, including XPS. A special generic nanostructure was then considered as the source of the anomaly. The micrographs on the three different films presented in that paper have quite distinct features but each clearly shows some isolated gold surrounded by the conducting network to which it is not connected. With the insulator ring empty, the common peak position is estimated using the gold data used in figure 3(b) to be at f = 0.88 or r/R = 0.94. The Au core-void ring entities as imaged were 30 to 40nm across with the empty "ring" 1 to 2 nm thick. These relative dimensions are in close accord with theestimated peak position. The detailed shape of the absorptance peak involves an admix of neighbouring f values, which as was pointed out, are unavoidable in these randomly grown structures. For example in silver a change from f = 0.92 (or r/R = 0.959) to f = 0.94 (r/R = 0.969)

shifts the resonance peak by 200 nm. Once the voids are filled with an insulator this sensitivity is enhanced, as all resonances then shift to longer wavelength.

The second piece of evidence comes from a careful re-examination of optical responses in a very well known and much studied system, growing silver and gold films deposited in vacuum [1, 3, 9]. The anomalous absorption of interest here appears quite strongly just above the percolation threshold. It is in a narrower mass thickness zone in Ag than in Au, and hence is easier to identify in gold films. Most published spectral data in this regime has been limited to transmittance and reflectance, and theoretical modelling has assumed a common nanostructure throughout of either islands or a conducting network. Such treatments led to the additional transition entities and their optical anomalies not being picked up. When spectral absorptance is extracted for mass thicknesses near percolation, these anomalous peaks appear. For example if the thin film gold data in some films in reference [1] is processed they appear near 0.9 μm just as in mesoporous gold. Measured $n^*(\lambda)$, $k^*(\lambda)$ values for the special class of films near the percolation threshold also gave anomalies in the wavelength range just where the metal-in-metal absorption peaks occur. Attempts to model them failed in the past, but equation (3) provides an explanation.

To add novelty to the bank of historical data and stronger evidence of these anomalies we have looked at similar silver layers under an oxide film. This does bring out the anomalies more clearly. Their reduced strength and position at shorter wavelength in the historical optical data may be another reason they were not picked up in the past. The absorption peak with oxide rings in place of voids for a range of Ag mass thicknesses just above percolation is always centred in data to date in films of different silver mass thickness at 1.0 eV (1.24 μm). This is for nanoporous silver buried under a fixed insulating oxide layer. An example of measured silver absorptance in an oxide/silver/oxide film stack with the silver layer just above the percolation point is in figure 4. We have many more examples of such peaks. The Ag was sputtered to a 6.4 nm mass thickness in this sample before adding the oxide layer. It is this data we will model. This peak weakens and eventually vanishes as more mass is added. This is expected as the isolated islands involved progressively join up with the network as mass is added. All peaks, though of varying intensity,

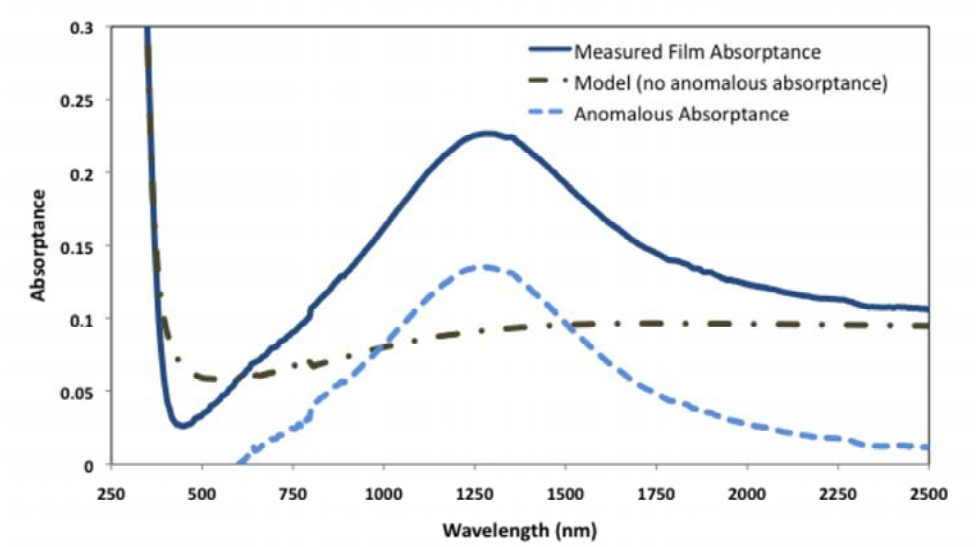

Figure 4 Anomalous absorption peak in a thin silver layer between oxides of index 2.0. To quantify and separate off the anomalous peak (dashed) the background absorption of the surrounding inhomogeneous conductor is first modelled (dot-dash) as shown, then subtracted from the total absorptance.

lie at the same 1.0 eV frequency. As with gold this silver peak cannot be explained by any variations to the silver energy bands. It is broadened because there is an admix of f values contributing as can be expected from the micrographs such as that in figures 5 and 6.

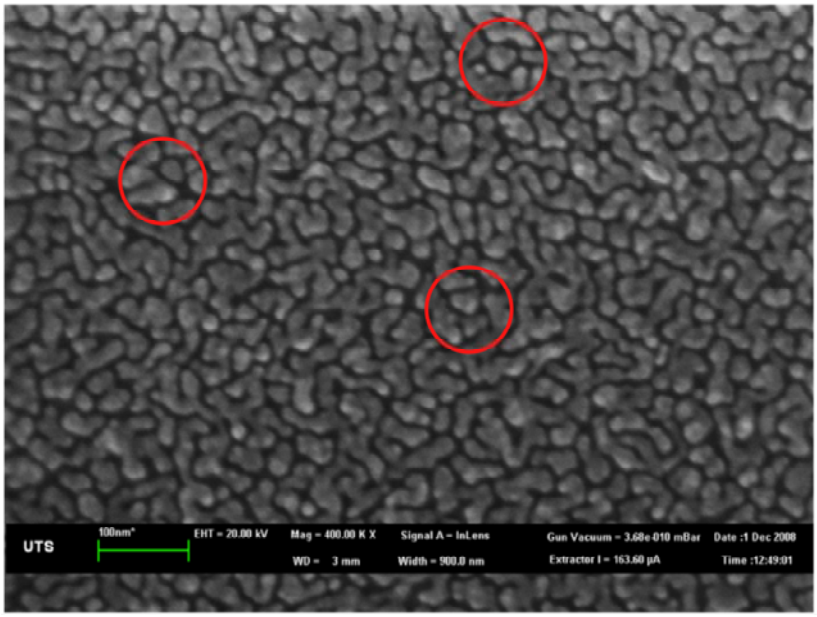

Figure 5 A thin silver layer just above percolation. Potential resonant candidates circled.

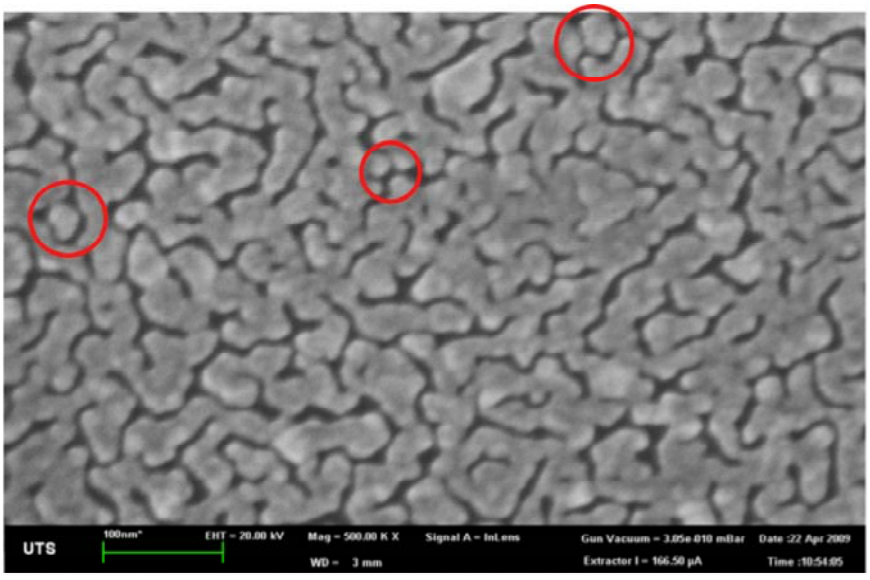

Figure 6 A thin silver layer further above percolation, than the example in figure 5. It is close to the layer on which absorptance data is presented in figure 4. Example potential candidates circled. NIR optical response is Drude like apart from the special resonances

The observed anomalous absorptive response shown in the dashed line in figure 4 is for a buried layer close in structure to that shown in figure 6. This is testimony to the strength of these metal/oxide shell/metal SP resonances as there appear to be a low density of such "special"

islands. Strong absorptance with very low concentrations of conducting nanoparticles is a signature of isolated nanoparticle SPR. For example 0.02% of LaB_6 nanoparticles in 0.7 mm of PVB yield similar NIR attenuation [13] to that in the figure 3 this system. These metal films are thin so the entities of interest must be strongly resonant.

4. Discussion

To understand and fit the absorption peak in figure 4 it is first necessary to model the resonances when the voids are filled with oxide. A set of spectra like those in figure 2 arise, except each f value peak is shifted to much longer wavelength. For example at f = 0.85 with just void insulating rings the resonance peaks at 740 nm but with oxide rings it is at 1370 nm. Since we have experimental k*(λ) data on this layer the model plot of k*(λ) is presented for q = 0.05 to give a direct comparison to the observed k*(λ). It is also easy from this plot to gauge where the sequence of absorption peaks lie. We first deal with the observed peak position, then the complete absorption band.

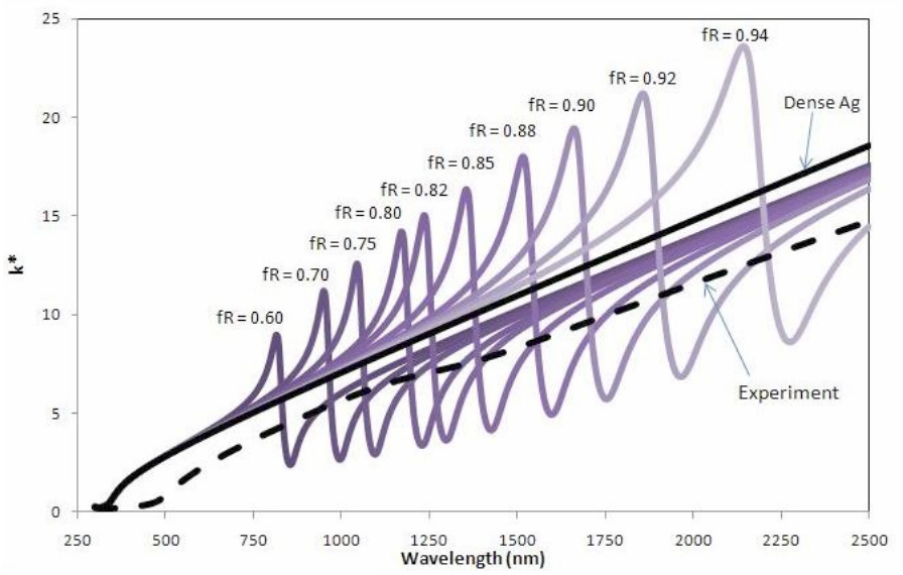

Figure 7. Imaginary part of refractive index k* (dashed) in an experimental conducting nanoporous network coated with oxide as a function of wavelength compared to that in dense silver (unbroken). The set of resonance plots is for the structure in figure 1 with the rings having refractive index of the overlayer n = 2.0.

The peak in figure 4 is just over 1.0eV at 1,250 nm. The oxide ring-in-silver resonance with this peak value is at f = 0.83 or at (r/R) = 0.91. From the image in figure 6 we estimate that the average entity of interest within the conducting network has diameter in the range 26 to 28 nm and core isolated island diameter in the range 24 to 26 nm. Thus if r = 12.5 nm and R = 13.5 nm then f = 0.86 which is close to the theoretical f value at the observed peak wavelength. The insulating annulus wall thickness leading to this peak position is close to 1 nm if f = 0.86. It is interesting that our earlier reported anomalous gold peak in mesoporous gold has a similar f value of 0.88 at its peak [5,11]. It is however at a much lower wavelength than this buried silver layer due to the ring being void. This common structural feature of average f near 0.85, must ultimately link to the way these porous network structures grow, which is dictated by diffusion-limited aggregation. This in turn leads to linked structures with a universal fractal dimension [14]. Our result indicates diffusion limited aggregation will lead in general to isolated “residues” of the

starting structure within the main matrix at intermediate stages of network growth. A universal structural character thus arises as the network evolves but the anomalous resonances we observe means that not all material belongs to the core fractal backbone at densities just past the percolation threshold.

To reproduce the broader absorption spectrum in figure 4 and the experimental k*(λ) in fig. 7 we invoke a distribution of resonances, which are expected from the images and the resonance sensitivity to small changes in f. Because peak intensity falls as resonance wavelength falls, while the peak in figure 4 is fairly symmetric a larger number of smaller f value entities may be present. They are however very weak or absent in experiments and in models. $f < 0.6$ ($r/R = 0.78$) and $\lambda < 600$ nm as seen in figures 4 and 7 can thus be neglected. Weighting the individual f spectra to reproduce the observed absorption spectra leads to a plot like that in figure 8, but the influence of low f inclusions is weak.

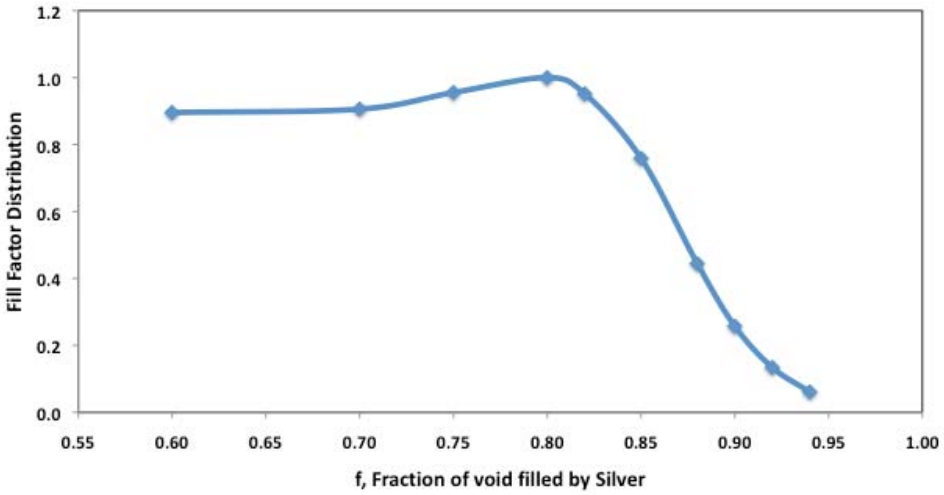

Figure 8 Distribution of resonant entity fill factor $f_R = (r/R)^2$ for silver as needed to reproduce the observed absorption spectra in figure 4.

The falloff for $f > 0.85$ is expected and it is unlikely that many examples exist with $f > 0.90$ (which implies $(r/R) > 0.95$.) With the total entity having R around 14 nm, the annulus thickness (R–r) would then be less than 0.7 nm. At the $f = 0.6$ cut-off (R-r) ~ 3 nm in this system. Thus the distribution in figure 8 covers a range of insulator wall thicknesses from 3 nm to 1 nm, which is in keeping with SEM images. The result is a range of individual overlapping resonances confined mainly to the range 700 nm to 1800 nm. If one makes a weighted sum of the individual resonances in figure 7 with the distribution in figure 8 this leads semi-quantitatively to the observed dashed plot in figure 4. The observed k*(λ) curve has two contributions that lower it relative to the dense silver in figure 7; one is from the underlying porous matrix and one from the combination of resonances from figs. 7 and 8 that also yield the absorptance plot in figure 4. The noticeable kink in k*(λ) near 1200 nm occurs close to the resonance peak. This kink has never been adequately explained until now. A final small adjustment of q can provide an almost exact fit to k* (λ) with q close to 0.05. q also evolves with thin film growth. This is an interesting but more complex story involving a refinement to continuum percolation theory.

To achieve any of the intriguing dielectric responses with less disperse f values as seen in figures 2 and 3, and the resulting quite novel spectral reflectance and absorptance plots they lead to, requires engineering of rings within the metal with a limited spread of wall thickness and values of this thickness around 1 to 3 nm if R < 30 nm. Larger diameter cores would enable thicker walls for the same f value.

Production of such 2d structures on a small scale in films ~ 10 nm thick may be feasible with e-beam etching or e-beam lithography, and possibly by ion beam etching. The strong resonant response means a large areal density is not needed. For larger areas nano-indentation of suitable patterns may be feasible, directly or in an overlayer for subsequent etching. Narrow resonances could be invoked in thin films starting with dilute layers of metal nanoparticles with limited dispersion in diameter. They can be vacuum overcoated with a thin insulating layer, then vacuum coated with metal. This thin film's effective optical constants emerge from a 3-d version of the models used in this treatise. Films using pre deposited metal nanoparticles have been made.

For 3-d particles in other metal formats another approach might be to use a higher melting point metal as the core nano-sphere. It could be pre-coated with a refractory oxide and dispersed in a lower melting point molten meta, which is then solidified. Hetero-metal systems with a different core metal to the matrix metal can be modelled with simple variations of the models introduced in this paper. A low density random system could be made by mixing a low number of the insulator coated metal nanospheres with refractory insulator spheres, before filling in to form the conducting network.

5. Conclusion

Tunable surface plasmon resonance can occur on a metal nanoparticle inside a metal or within a porous conducting network, provided a thin insulator layer separates the two plasmonic materials. This resonance structure can arise naturally during growth in thin conducting layers just beyond the percolation threshold, and in mesoporous metal layers made by etching. In growing metal layers a residual nano-island of metal is cut-off from the surrounding conducting network by a loop of insulator or void. This resonant feature is enhanced and strongly red shifted when insulating oxide replaces void. A model representing the average resonant element by a circular cylinder of metal inside a circular insulating annulus is capable of describing the anomalous NIR absorption feature found in select nanoporous silver and gold films. Insulator wall thickness from 1 to 3 nm are present. This study has focussed on naturally occurring electrically isolated metal in porous conductor structures. Follow up work involved engineered nanostructures buried in dense metal whose optical response systematically confirms other key features of the model predictions presented here and proves the resonance can be made to occur within dense metal. The ability to engineer quite novel spectral response within a dense metal opens a door to many new possibilities in plasmonics.

Acknowledgements Pilkington/NSG Pty Ltd partially supported this work. Dr John Ridealgh of Pilkington/NSG UK Technical Centre, supplied key samples and valuable insights. Geoff McCredie, Abbas Maaroof, Mike Cortie and Angus Gentle were involved in relevant prior studies on nanoporous films and gave useful comments on this work.

References

[1] Smith G B, Niklasson G A, Svensson J S E M and Granqvist C G 1986 Noble -metal- based transparent infra-red reflectors: Experiments and theoretical analyses for very thin gold films *J. Appl. Physics* **59** 571-581
[2] Bertier S, Peiro J, Fagent S and Gadenne P 1997 Infrared absorption of granular metal films in the percolation range *Physica A* 241 1-5
[3] Seal K, Nelson M A, Ying Z C, Genov D A, Sarychev A K and Shalaev V M 2003 Growth, morphology and optical and electrical properties of semicontinuous metallic films *Phys. Rev. B.* **67** 035318 1-13
[4] Smith G B, Gentle A R and Maaroof A I 2007 Metal insulator composites which act optically like homogeneous conductors *J Nanophotonics* (SPIE Digital Library) **1** 013507
[5] Maaroof A I, Gentle A R and Smith G B 2007 Bulk and Surface Plasmons in Highly Nanoporous Gold Films *J.Phys D* **40** 5675-5682
[6] Oldenberg S J Blaaderen A van, and Halas N 1998 Nanoengineering of optical resonances *Chem Phys. Letters* **288** 243-247
[7] Graf C and Blaaderen A van, 2002 Metallodielectric colloidal core-shell particles for photonic applications *Langmuir* **18** 524-534
[8] Schelm S and Smith G B 2005 Internal Electric Field Densities of Metal Nanoshells, *Journal of Physical Chemistry B* **109** 1689 - 1694
[9] Maaroof A I and Smith G B 2005 Effective optical constants of nanostructured silver films and impact of an insulating overlayer *Thin Solid Films* **485** 198 – 206
[10] Palik E D, *Handbook of optical constants of solids* (Academic, 1985)
[11] Smith G B, Maaroof A I and Gentle A Homogenized 2007 Lorentz-Drude optical response in highly nanoporous conducting gold layers produced by de-alloying *Optics Communications* **271** 263-268
[12] Maaroof A I, Cortie M B, Gentle A and Smith G B 2007 Mesoporous gold sponge as a prototype meta-material *Physica B* **394** 167 – 170
[13] Schelm S and Smith G B 2003 Dilute LaB_6 nanoparticles in polymer as optimised clear solar control glazing *Appl. Phys. Lett.* **82** 4346-4348
[14] Smith G B, Maaroof A I and Cortie M B 2008 Percolation in nanoporous gold and the Principle of Universality from two dimensions to hyperdimensions *Phys. Rev B.,* **78** 165418 (11pp)